International Journal of Applied Pharmaceutics

ISSN- 0975-7058 Vol 16, Issue 4, 2024

Original Article

GC-MS ANALYSIS AND IN SILICO APPROACHES OF *INDIGOFERA PROSTRATA* AND *LANTANA CAMARA* CONSTITUENTS FOR ANTI-ALZHEIMER STUDIES

NEELAM INJETI[1], KUMAR SHIVA GUBBIYAPPA[2*]

[1]GITAM Deemed to be University, Gandhi Nagar, Rushikonda, Visakhapatnam-530045, Andhra Pradesh, India. [2]GITAM School of Pharmacy, GITAM Deemed to be University, Rudraram, Patancheru Mandal, Hyderabad-502329, Telangana, India
[*]Corresponding author: Kumar Shiva Gubbiyappa; [*]Email: sgubbiya@gitam.edu

Received: 17 Mar 2024, Revised and Accepted: 18 May 2024

ABSTRACT

Objective: The present investigation explored the binding affinities of phytoconstituents present in *Indigofera prostrata* and l*antana camara* that acted as Anti-Alzheimer's drug. Also the phytoconstituents were identified by Gas chromatography–Mass spectrometry (GC-MS) against selected targets, i. e., β-amyloid and acetylcholinesterase (AchE).

Methods: *I. prostrata* seeds and leaves of l. *camara* were macerated using methanol as a solvent, then analysed for phytoconstituents through GC–MS. The Chromatogram revealed the presence of 14 in *I. prostrata* and l. *camara* 19 novel phytoconstituents. These phytoconstituents were explored for their Anti-Alzheimer's effect by iGEMDOCK software against selected targets, namely recombinant human acetylcholinesterase β-amyloid (protein data bank ID: 2LMN).

Results: The docking analysis resulted in four and five phytoconstituents with the highest binding affinity towards the selected targets in *I. prostrate* and l. *Camara, I,* respectively. The bioactive compounds present in the methanolic extract of l. *camara* were, Heptane,4-ethyl-2,2,6,6-tetramethyl-'N, N-Dinitro-1,3,5,7-tetrazabicyclo[3,3,1] nonane, Spiro[androst-5-ene-17,1'-cyclobutan]-2'-one,3-hydroxy-,(3. beta,17. beta.). ligPlot depicted hydrophobic bonds, hydrogen bonds, and their bond lengths in each of the *in silico* effective docking compounds, which were compared with their respective standards.

Conclusion: From the results obtained it was concluded that the *in silico* analysis using computational approaches might become a prospective novel compound against the selected targets in Alzheimer's disease.

Keywords: *Indigofera prostrata, lanata camara,* 2LMN, Campesterol, Stigmasterol, γ-Sitosterol, Lupeol

DOI: https://dx.doi.org/10.22159/ijap.2024v16i4.50890 Journal homepage: https://innovareacademics.in/journals/index.php/ijap

INTRODUCTION

The most common cause of dementia is Alzheimer's disease (AD), a retrogressive brain illness. It is always associated with memory-related problems, difficulty in delivering language, inability to solve problems, and other typical deterioration in mental ability, eventually affecting an individual's potential to carry out daily tasks [1]. The demolition of neurons in the brain region imputesa detrimental effect on cognitive function. The fundamental body activities like walking and swallowing deteriorate slowly, then ultimately, individuals who are nearing the end of the illness are bedridden and need 24 h care. AD ultimately results in death. There is a significant socioeconomic burden globally in the upcoming years, as a result of the aged population. As per the World Health Organization, accounting for 60–80% of cases around the world, AD is the most common type of dementia, costing an estimated US$818 billion affecting around 47 million people worldwide [2]. Oxidative stress has been linked to the pathophysiology of AD and can result from metal buildup or damage to neurons. To overcome the limits of present therapies for AD, extensive research is being conducted to explore medications that are both effective and devoid of unwanted side effects. In this regard, naturally occurring dietary polyphenolic phytochemicals have drawn a lot of importance as potential substitute treatments for AD. The World Alzheimer's Report 2019 estimates that 50 million people worldwide are affected by dementia. By 2050, this fig. will have doubled every 20 years to 152 million. The primary pathogenic characteristics were aberrant Aβ deposition and hyperphosphorylated tau protein accumulation that resulted in nerve fibre tangles. Currently, cholinesterase inhibitors are frequently used to help AD patients with their cognitive function, but they are only able to slow the disease's progression [2, 3].

In diseases with complex pathogenesis, the study of the "multi-component, multi-target" drug action mechanism plays a prominent role. As a multi-component and multitarget discipline system, network pharmacology has unique advantages in studying complex molecular mechanisms [4]. According to many studies, acetylcholine (ACh), a neurotransmitter involved in the encoding of new memories and information, is depleted, which leads to memory impairment. Consequently, the current paradigm for treating AD involves blocking acetylcholinesterase (AChE) enzymes [5]. On the contrary, few medications that inhibit β-amyloid and AChE, can momentarily alleviate symptoms but have detrimental side effects. Pathophysiologically, AD may involve the deposition of a β protein in neurofibrillary tangles and the synthesis of the AChE enzyme in cholinergic synapses, based on analysis of brain samples conducted through biochemical and histological research. Use of cholinesterase inhibitors approved by US Food and Drug Administration (FDA) for the treatment of memory-related diseases [6]. However, these medications can have adverse effects at high doses, such as hepatotoxicity, decreased appetite, nausea, vomiting, and diarrhea [7].

Molecular docking studies may now be conducted using programs on various methods, which have increased the utility of docking as a tool in pharmaceutical research. Due to the very complex nature of Alzheimer's disease, a multi-target/multi-drug approach may be more successful than traditional monotherapy [8]. This enabled few researchers to use a computational method to identify approved drug combinations that may reduce microglial inflammation in AD more effectively than individual treatments. Drug discovery for multi-targeted therapy presented new hardships. These may include the ability to cross the blood-brain barrier, optimal ADMET characteristics, no off-target side effects, and excellent binding affinity of ligands for various targets [9]. As computational approaches are effectively used for single-target drug development projects, these obstacles may be overcome by *in silico* methodologies for an effective solution in less time and money [10].

In this work, a virtual screen of several tacrine compounds was examined using a molecular docking technique, with the AchE crystal structure serving as a receptor [11]. The objective of this approach was to detect a putative lead ligand that might serve as a

model for creating hypothetical compounds with higher binding scores and more noteworthy chemical interactions with the receptor. Two herbal drugs were selected by name-*Indigofera prostrate* (Fabaceae) and l*antana camara* (Verbenaceae)in the present study. *I. prostrata* has spread branches with unique features that make it a promising candidate for perennial crops [12]. Different species differ greatly from one another; this variation includes differences in fruit type, flowering shape, and pericarp thickness. l. *Camara* is a flowering plant native to American tropics, distributed throughout India, and resides in places with moderate to high summer rainfall. Since ancient times, it has been used as a traditional medicine used as anti-bacterial, anti-fungal, anti-motility, anti-ulcerogenic and anti-hyperglycemic activity [13]. It also sought to find a probable ligand that would serve as a model for creating imaginary compounds with higher binding scores and exceptional interactions with the receptor.

MATERIALS AND METHODS

Plant material

From the nearby locations of Tirupati, seeds of *I. prostrata* and leaves of l. *Camara* were obtained and were authenticated by Dr. K. Madhava Chetty M. Sc., Ph. D, and the specimen was preserved with voucher number P403 and P424.

Extraction by maceration

Fresh seeds of *I. prostrata* and leaves of l. *camara* were cleaned with water and shade-dried, then grounded to coarse powder. About one kg of the material was immersed in methanol and stored for seven days, stirring occasionally, to allow the maceration process. Then the content was filtered and evaporated at 40 °C on 8 d, then placed in desiccator to eliminate the solvent. The dried material was used for further studies [14].

Preliminary phytochemical analysis

The test extracts were analysed for the existence of primary metabolites, such as carbohydrates, amino acids, proteins, and lipids, and secondary metabolites, like alkaloids, tannins, phenols, flavonoids, saponins, steroids, glycosides, and resins by means of standard methods [14].

Preparation of protein structure

The protein database was selected from https://www.rcsb.org/, and the AD receptor structures of Aβ (2LMN) was obtained from the above link. A virtual screening tool was used from https://pyrx.sourceforge.io/ and the receptor structures were screened [15-17].

Ligand preparation

The ligands discovered in GC-MS were shown using the newest version software ChemDraw 19.1 (PerkinElmer, Waltham, Massachusetts, United States). The ligand preparation had steps involved–conversions, corrections, structural adjustments, removal and optimization of lead. GC–MS detected ligand structures were drawn. The process of ligand preparation involved various steps–conversions, corrections, structural adjustments, removal and optimization of lead [18]. Finally, every prepared ligand was transformed into a three-dimensional (3D) PDB file format and preserved.

Docking analysis

By retaining the ligands in their rigid and varied conformations and poses, the binding energy of the ligands with the target receptor protein was assessed. It involved the computer analysis of relevant protein ligands together in 3D space. The specifications of 2.50 GHz Intel (R) Core (TM) i5 Intel Corp., Windows 10, Microsoft Corp. iGEMDOCK docking program were obtained from http://gemdock.life.nctu.edu.tw/dock/igemdock.php; also the modeling results were located. In the methanolic extract of *I. prostrata* and l. *camara* a protein structure of the receptor was docked that was identified with the phytoconstituents. For effective results, a stable standard dock was used. With the use of pharmacological interactions, iGEMDOCK provides an interactive tool for predicting the binding site and ligand docking status, tracking the advancement of integrated virtual screening, post-screening analysis (hierarchical tree view), and, in the end, providing the docked structure's binding energy. From https://discover.3ds.com/discovery-studio-visualizer-download, BIOVIA Discovery Studio Visualizer, a leading visualization tool was obtained to analyse binding site observations [19].

In silico ADME analysis

The compounds with a remarkable structural backbone underwent in silico ADME experiments conducted by the admetSAR server in order to assess their drug-likeness properties and thereafter be the focus of further investigation. The absorption, distribution, metabolism, and excretion characteristics that are critical for forecasting novel phytoconstituents with improved pharmacokinetic and pharmacodynamic activity were shown by ADME investigations. By using https://cactus.nci.nih.gov/translate/SMILES, translation was done [20].

The top five ligand smiles were uploaded on the admetSAR web server using http://lmmd.ecust.edu.cn/admetsar2/. The predicted result consists of intestinal absorption, carcinogenicity, acute oral toxicity and blood-brain barrier permeation.

LigPlot analysis

Academic license of ligPlot software obtained from https://www.ebi.ac.uk/. This is used to provide a 2-D representation of protein–ligand interactions, intermolecular interactions like hydrogen bonding, hydrophobic interactions and atom accessibilities of their strengths [21].

RESULTS

The test extracts MEIP and MELC were analysed for the presence of phytochemical constituents like carbohydrates, amino acids, proteins, alkaloids, cardiac glycosides, triterpenoids, saponins, flavonoids, phenolic compounds, tannins, steroids and gums.

Fig. 1 represented a chromatogram of GC-MS of MEIP, while table 1 was depicted with the retention time (RT), atomic equation, molecular weight (MW) and area (%) of the phytochemical constituents. The bioactive compounds were 1-Butanol, 3-methyl-, formate, d-Mannose, β-Acorenol, 3-O-Methyl-d-glucose, Hexadecanoic acid, methyl ester, n-Hexadecanoic acid, Phytol, E-8-Methyl-9-tetradecen-1-ol acetate, Hexadecanoic acid, 2-hydroxy-1-(hydroxymethyl)ethyl ester, 9,12-Octadecadienoic acid (Z,Z)-, 2-hydroxy-1-(hydroxymethyl)ethyl ester, Campesterol, Stigmasterol, γ-Sitosterol and lupeol.

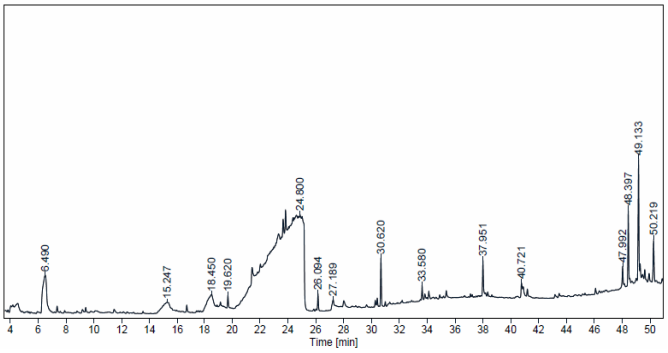

Fig. 1: GC-MS chromatogram of methanolic extract of *I. prostrata* (MEIP)

Table 1: Bioactive compounds of methanolic extract of *I. prostrata* (MEIP)

S. No.	R. Time (Min)	Area (%)	Compound name	Molecular formula	Molecular weight (g/mol)	Structure of the compound
1	6.494	19.34	1-Butanol, 3-methyl-, formate	$C_6H_{12}O_2$	116.16	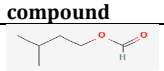
2	15.246	8.06	d-Mannose	$C_6H_{12}O_6$	180.156	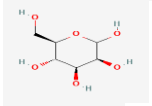
3	19.621	0.59	β-Acorenol	$C_{15}H_2O_6$	222.37	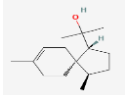
4	24.797	7.55	3-O-Methyl-d-glucose	$C_7H_{14}O_6$	194.18	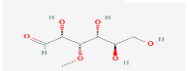
5	26.091	1.56	Hexadecanoic acid, methyl ester	$C_{17}H_{34}O_2$	270.5	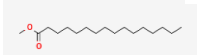
6	27.191	6.49	n-Hexadecanoic acid	$C_{16}H_{32}O_2$	256.42	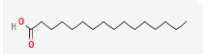
7	30.623	4.70	Phytol	$C_{20}H_{40}O$	296.5	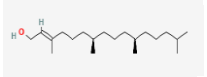
8	33.580	0.79	E-8-Methyl-9-tetradecen-1-ol acetate	$C_{17}H_{32}O_2$	268.4	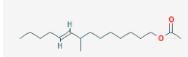
9	37.950	4.11	Hexadecanoic acid, 2-hydroxy-1-(hydroxymethyl)ethyl ester	$C_{19}H_{38}O_4$	330.5	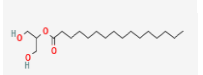
10	40.719	5.43	9,12-Octadecadienoic acid (Z,Z)-, 2-hydroxy-1-(hydroxymethyl)ethyl ester	$C_{21}H_{38}O_4$	354.5	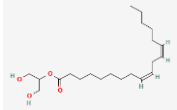
11	47.989	1.21	Campesterol	$C_{28}H_{48}O$	400.7	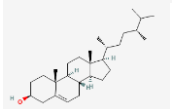
12	48.395	6.42	Stigmasterol	$C_{29}H_{48}O$	412.7	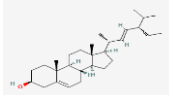
13	49.133	12.59	γ-Sitosterol	$C_{29}H_{50}O$	414.7	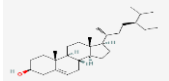
14	50.214	8.35	Lupeol	$C_{30}H_{50}O$	426.7	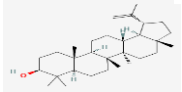

Fig. 2 represented the chromatogram of GC-MS of MEIP, while table 2 was depicted with RT, atomic equation, MW and area (%) of the phytochemical constituents. The bioactive compounds present in the methanolic extract of l. *camara* were, Heptane,4-ethyl-2,2,6,6-tetramethyl-'N, N-Dinitro-1,3,5,7-tetrazabicyclo[3,3,1] nonane, Spiro[androst-5-ene-17,1'-cyclobutan]-2'-one,3-hydroxy-,(3. beta,17. beta.)-

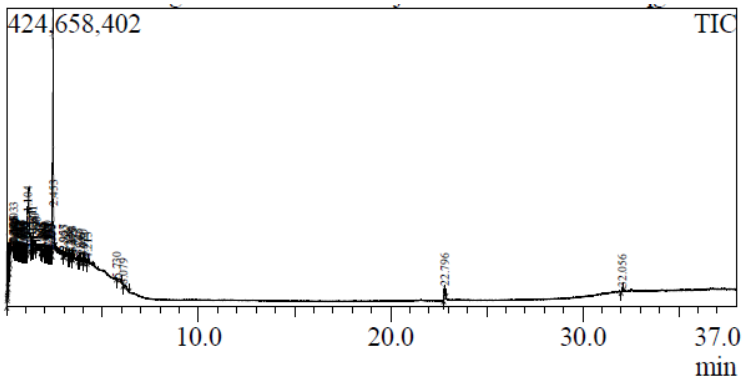

Fig. 2: GC-MS chromatogram of methanolic extract of l. *camara* (MELC)

Table 2: Bioactive compounds of methanolic extract of l. *camara* (MELC)

S. No.	R. Time (Min)	Area (%)	Compound name	Molecular formula	Molecular weight (g/mol)	Structure of the compound
1	0.033	6.59	2-Oxetanone, 4,4-dimethyl-	$C_5H_8O_2$	100	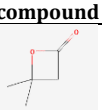
2	4.213	0.18	Difluorinemonoxide	F_2O	54	
3	2.957	0.41	Nitrosyl chloride	ClNO	65	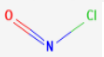
4	0.860	0.87	Ethane, 1-chloro-1-fluoro-	C_2H_4ClF	82	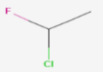
5	0.765	0.11	Carbonic chloride fluoride	CClFO	82	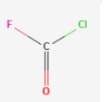
6	1.104	20.93	Tetraborane (10)	B_4H_{10}	54	
7	1.321	5.22	1-Propene,3-fluoro-	C_3H_5F	60	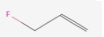
8	1.371	2.12	Heptane,4-ethyl-2,2,6,6-tetramethyl-	$C_{13}H_{28}$	184	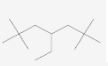
9	1.480	2.05	1-Decene,2-methyl-	$C_{11}H_{22}$	154	
10	3.849	0.26	N, N-Dinitro-1,3,5,7-tetrazabicyclo[3,3,1]nonane	$C_5H_{10}N_6O_4$	208	
11	2.224	0.18	2H-Pyran-2,6(3H)-dione,dihydro-	C5H6O3	114	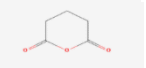
12	2.453	13.90	Benzene,1-(chloromethyl)-2-nitro-	$C_7H_6ClNO_2$	171	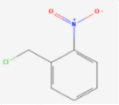
13	2.995	0.63	Methanamine, N,N-dimethyl-, compd. withtriborane(7) (1:1)	$C_3H_{16}B_3N$	99	
14	3.980	0.32	2-Oxetanone, 4-methylene-	$C_4H_4O_2$	84	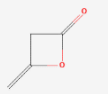
15	4.022	0.20	Propane,1-chloro-	C_3H_7Cl	78	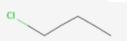
16	5.730	1.99	Carbonochloridic acid, propyl ester	$C_4H_7ClO_2$	122	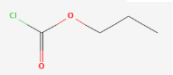
17	6.079	1.64	Propanenitrile, 2,2-dimethyl-	C_5H_9N	83	
18	22.796	2.90	Oxirane, decyl-	$C_{12}H_{24}O$	184	
19	32.056	0.88	Spiro [androst-5-ene-17, 1'-cyclobutan]-2'-one, 3-hydroxy-, (3. beta, 17. beta.)-	$C_{22}H_{32}O_2$	328	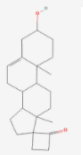

Molecular docking analysis

Preparation for ligands

In the methanolic extract of *I. prostrata* and l. *camara* the structures of the ligands were identified by GC–MS as depicted table 1 and table 2.

Docking analysis

The identified ligands by GC-MS in the test extracts that targeted Aβ protein and AChE of AD were represented with their respective binding energies, also the interaction of active compounds present with their respective proteins was presented.

Top docking score 2LMN interaction with phytoconstituents

In the methanolic seed extract of *I. prostrata* four phytoconstituents namely campesterol, Stigmasterol, γ-Sitosterol and lupeol exhibited highest binding affinity, whereas the methanolic leaf extract of*L. camara* indicated with the five highest binding affinity compounds-Carbonochloridic acid, propyl ester, Propanenitrile, 2, 2-dimethyl-,

Oxirane, decyl-, Spiro [androst-5-ene-17, 1'-cyclobutan]-2'-one, 3-hydroxy-, (3. beta, 17. beta.)-and2-Oxetanone, 4-methylene-respectivelyas comparable to the standard Curcumin (−110.2 kcal/mol).

In silico ADMET prediction of MEIP and MELC

The ADME properties of MEIP (table 3 and fig. 3) and MELC (table 4, fig. 4, fig. 5) like intestinal absorption; blood-brain barrier permeation, was identified for the selected ligands which were targeted in AD.

Table 3: *In silico* ADMET prediction of the top four compounds in MEIP

Selected compounds	Dock score	Intestinal absorption	BBB permeation	Carcinogenicity
Campesterol	-7.3	+	+	-
Stigmasterol	-6.4	+	+	-
γ-Sitosterol	-9.6	+	+	-
Lupeol	-8.4	+	+	-

+indicates positive impact;-indicated negative impact

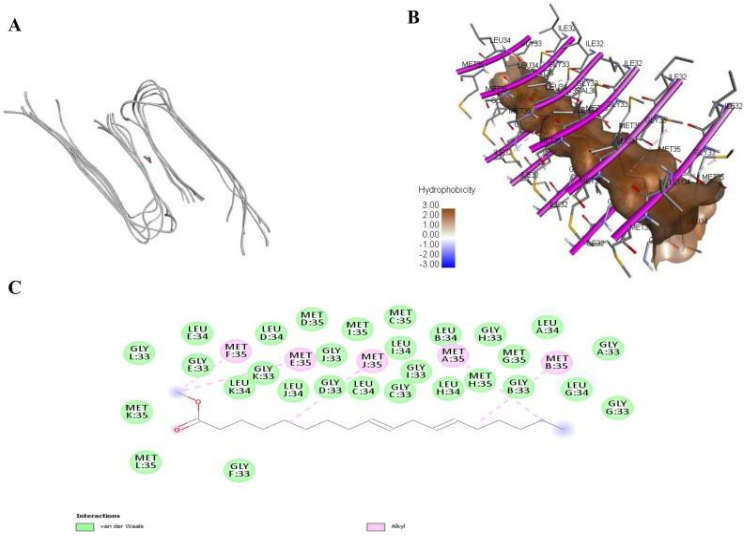

Fig. 3: 2LMN interacting with γ-Sitosterol. A) Docking chain view, B) ligand binding pockets, C) 2D view of active binding sites

Table 4: *In silico* ADMET prediction of the top five compounds in MELC

Selected compounds	Dock score	Intestinal absorption	BBB permeation	Carcinogenicity
Oxirane, decyl-	-7.3	+	+	-
Propanenitrile, 2,2-dimethyl-	-6.4	+	+	-
Propyl ester,	-9.6	+	+	-
Carbonochloridic acid,	-8.4	+	+	-
Spiro [androst-5-ene-17, 1'-cyclobutan]-2'-one, 3-hydroxy-, (3. beta, 17. beta.)-	-9.8	+	+	-

+indicates positive impact;-indicated negative impact

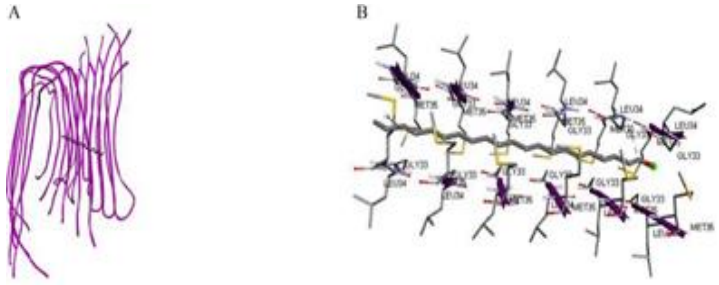

Fig. 4: Molecular docking views: (A) Chain 2LMN interacting with Spiro [androst-5-ene-17, 1'-cyclobutan]-2'-one, 3-hydroxy-, (3. beta, 17. beta)

LigPlot analysis

LigPlot depicted hydrophobic bonds, hydrogen bonds, and their bond lengths in each of the *in silico* effective docking compounds, which were compared with their respective standards as mentioned in table 5 and fig. 3 in MEIP. It was detected that the ligand γ-Sitosterol with 2LMN interaction had 30 hydrophobic contacts with amino acid residues like Gly C: 33, Gly I: 33, Gly K: 33, leu J: 34, Met

K: 35, leu E: 34, Gly F: 33, Gly G: 33, Gly E: 33, leu I: 34, Met F: 35, Gly B: 33, Met E: 35, leu H: 34, leu C: 34, Gly J: 33, leu D: 34, Met C: 35, leu G: 34, Met J: 35, leu K: 34, Gly H: 33, leu B: 34, Gly D: 33, Met G: 35, leu A: 34, Gly l: 33, Met A: 35, Met H: 35, Gly A: 33 and without any H-bond interactions.

LigPlot depicted hydrophobic bonds, hydrogen bonds, and their bond lengths in each of the *in silico* effective docking compounds, which were compared with their respective standards as mentioned in table 6 and Fig. 5 in MELC. It was detected that the ligand Spiro [androst-5-ene-17, 1'-cyclobutan]-2'-one, 3-hydroxy-, (3. beta, 17. beta.)-with 2LMN interaction has 27 hydrophobic contacts with amino acid residues like Gly33(A), Gly33(B), Gly33(C), Gly33(D), Gly33(E), Gly33(F), Gly33(G), Gly33(H), Gly33(I), Gly33(J), Gly33(K), Gly33(L), leu34(A), leu34(B), leu34(C), leu34(D), leu34(E), leu34(F), leu34(G), leu34(H), leu34(I), leu34(J), leu34(K), Met35(C), Met35(D), Met35(E), Met35(F), Met35(G), Met35(H), Met35(J), Met35(K) and without any H-bond interactions.

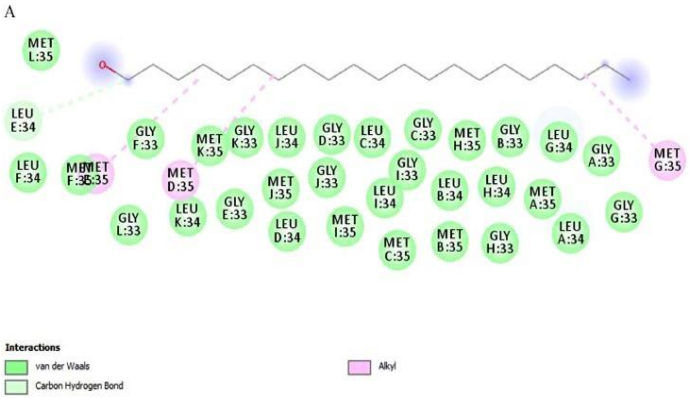

Fig. 5: 2D view of binding interaction: (A) Spiro [androst-5-ene-17, 1'-cyclobutan]-2'-one, 3-hydroxy-, (3. beta, 17. beta.)-

Table 5: Interactions of AD target protein amino acid residues with ligands at receptor sites by ligPlot analysis for MEIP

S. No.	Ligands	Amino acids involved and distance (Å)		
		Amino acid	Distance (Å)	Amino acid
1	γ-Sitosterol			Gly C: 33, Gly I: 33, Gly K: 33, leu J: 34,Met K: 35, leu E: 34, Gly F: 33, Gly G: 33,Gly E: 33, leu I: 34, Met F: 35, Gly B: 33,Met E: 35, leu H: 34, leu C: 34, Gly J: 33,Leu D: 34, Met C: 35, leu G: 34, Met J: 35,Leu K: 34, Gly H: 33, leu B: 34, Gly D: 33,Met G: 35, leu A: 34, Gly l: 33, Met A: 35, Met H: 35, Gly A: 33.
2	Standard Curcumin	Gln C: 15 His E: 13	2.61 3.12	Val E: 40, Glu F: 11, His B: 13, His F: 13, Val E: 39, Val F: 40, His C: 13, His D: 13.

Table 6: Interactions of AD target protein amino acid residues with ligands at receptor sites by ligPlot analysis for MELC

S. No.	Ligands	Amino acids involved and distance (Å)		
		Amino acid	Distance (Å)	Amino acid
1	Spiro [androst-5-ene-17, 1'-cyclobutan]-2'-one, 3-hydroxy-, (3. beta, 17. beta.)-			Gly33(A), Gly33(B), Gly33(C), Gly33(D), Gly33(E), Gly33(F), Gly33(G), Gly33(H), Gly33(I), Gly33(J), Gly33(K), Gly33(L), leu34(A), leu34(B), leu34(C), leu34(D), leu34(E), leu34(F), leu34(G), leu34(H), leu34(I), leu34(J), leu34(K), Met35(C), Met35(D), Met35(E), Met35(F), Met35(G), Met35(H), Met35(J), Met35(K).
2	Standard Curcumin	Gln C: 15 His E: 13	2.61 3.12	Val E: 40, Glu F: 11, His B: 13, His F: 13, Val E: 39, Val F: 40, His C: 13, His D: 13.

DISCUSSION

AD is characterized by gradual loss of neurons in the brain, deterioration in cognitive ability, and senile plaques. Although currently, AD drugs are used for symptomatic purposes, no medication is available to delay the development or avoid neuronal degeneration [22]. Aβ is normally present in the soluble form in CSF fluid and blood, but in AD patients, Aβ is fibrillated to form filamentous structures of insoluble Aβ in the brain, however, abnormal Aβ aggregation mechanism is not well known. Substantially, AD leads to the death of nerve cells, resulting in cognitive and behavioral decline. Since the most widely used existing medicines cannot successfully prevent or cure AD, it becomes vital to identify substances that can defibrillate Aβ fibrillation [23].

Recently, acetylcholinesterase inhibitors (AChEIs) like donepezil, tacrine, galantamine and rivastigmine have been included in the routine treatment for AD. Every drug presents some or the other adverse effects and may have drug-drug interactions, which show up fatality [24]. When these AChEIs were considered for the treatment of AD, they act by minimizing the progression of cognitive dysfunction and might be successful in the initial and intermediate stages of AD in a few patients. In searching for alternatives in the treatment of AD, many herbal products have been tried and used in the treatment of AD in an attempt to find alternatives, but the results have been inconsistent in terms of clinical response. The BBB stands in the way of many possible therapeutic substances entering the brain, making it the largest obstacle to drug delivery into the brain. Although taking the herbs orally is a popular method of administration, it is unclear from the available research whether the constituents of the herbs can enter the central nervous system through systemic circulation [25, 26].

In this study, methanolic seed extract of *I. prostrata* was subjected to GC–MS analysis and detected 14 novel phytoconstituents; the identification was done on the basis of their different retention times and MS data compared with WILEY8. lib and NIST14s. lib. Against the selected AD targets, 14 chemical constituents were screened [27, 28]. Based on the binding energy of these compounds, the top four phytoconstituents with the highest binding affinity and lowest

binding energy towards the Aβ target were identified as compared to the standard curcumin [26, 27]. The drug-likeness characteristics of the top five binding affinity compounds for both AD targets were screened from admetSAR prediction. The four phytoconstituents Campesterol, Stigmasterol, γ-Sitosterol and lupeol, were identified for their specific action on the Aβ target. The methanolic leaf extract of l. *Camara* was subjected to GC–MS analysis and was detected with19 novel phytoconstituents; identification was done based on their different retention times and MS data compared with WILEY8 [29, 30]. All these 19 chemical constituents were screened against selected AD targets. Based on the binding energies of these compounds, the top four phytoconstituents with the highest binding affinity and lowest binding energy towards the Aβ target were identified as comparable to the standard curcumin [31]. The drug likeness characteristics of the top five binding affinity compounds for both AD targets were screened from admetSAR prediction. Five phytoconstituents specific action on Aβ target were named as Oxirane, decyl-Propanenitrile, 2,2-dimethyl-, propyl ester, Carbonochloridic acid and Spiro [androst-5-ene-17, 1'-cyclobutan]-2'-one, 3-hydroxy-, (3. beta, 17. beta.)-.

These substances had low oral toxicity, superior blood-brain permeability, no carcinogenicity, and a high intestine absorption capacity. Based on simulation studies, the anti-Alzheimer's chemicals are presented here. To validate the computational conclusions any further, more experimental data may be required.

CONCLUSION

Several bioactive chemicals that are utilized to treat a variety of disorders are thought to be potentially found in medicinal plants. In the present study, using *in silico* molecular docking analysis, phytoconstituents present in *I. prostrata* and l. *Camara* were detected by GC–MS. In silico molecular docking studies, one kind of computer research, are therefore helpful in understanding the presence of phytoconstituents with binding affinities for the two AD targets that have been chosen. Reducing adverse effects, costs, and time in drug discovery is achieved by utilizing molecular docking analysis to virtually screen natural chemicals in search of lead molecules. Pharmacokinetic property-based ligand screening is crucial since it lowers the likelihood that most medicines will fail at the clinical stage. As a result, after more investigation, these nine probable natural compounds present in the test drugs might be recommended as viable medications for the treatment of AD because they have good pharmacokinetic qualities and binding energy to two AD receptors (2LMN). To create more effective AD medications, these discovered lead compounds can be further altered and improved, followed by *in vivo* studies.

FUNDING

Nil

AUTHORS CONTRIBUTIONS

NI completed the research work, execution, and writing. SKG did the work plan, review, and corrections. All authors agree with the submission and publication. All authors have read and agreed to the published version of the manuscript.

CONFLICT OF INTERESTS

Declared none

REFERENCES

1. Bukke VN, Archana M, Villani R, Romano AD, Wawrzyniak A, Balawender K. The dual role of glutamatergic neurotransmission in Alzheimer's disease: from pathophysiology to pharmacotherapy. Int J Mol Sci. 2020 Oct 9;21(20):7452. doi: 10.3390/ijms21207452, PMID 33050345.
2. Rees TM, Brimijoin S. The role of acetylcholinesterase in the pathogenesis of Alzheimer's disease. Drugs Today (Barc). 2003 Jan;39(1):75-83. doi: 10.1358/dot.2003.39.1.740206, PMID 12669110.
3. Sharma S, Nehru B, Saini A. Inhibition of Alzheimer's amyloid-beta aggregation *in vitro* by carbenoxolone: insight into mechanism of action. Neurochem Int. 2017 Sep;108:481-93. doi: 10.1016/j.neuint.2017.06.011, PMID 28652220.
4. Casey DA, Antimisiaris D, O'Brien J. Drugs for Alzheimer's disease: are they effective? P T. 2010 Apr;35(4):208-11. PMID 20498822.
5. Warner J, Butler R. Drugs for Alzheimer's disease. More effective agents are needed. BMJ. 2001 Nov 10;323(7321):1127-8. doi: 10.1136/bmj.323.7321.1127a, PMID 11725755.
6. Hope T, Keene J, Fairburn C, McShane R, Jacoby R. Behaviour changes in dementia. 2: Are there behavioural syndromes? Int J Geriatr Psychiatry. 1997 Nov;12(11):1074-8. doi: 10.1002/(sici)1099-1166(199711)12:11<1074::aid-gps696>3.0.co;2-b, PMID 9427091.
7. Chen GF, Xu TH, Yan Y, Zhou YR, Jiang Y, Melcher K. Amyloid beta: structure, biology and structure-based therapeutic development. Acta Pharmacol Sin. 2017 Sep;38(9):1205-35. doi: 10.1038/aps.2017.28, PMID 28713158.
8. Akshatha JV, Santosh Kumar HS, Prakash HS, Nalini MS. In silico docking studies of α-amylase inhibitors from the anti-diabetic plant leucas *ciliata* benth. and an endophyte, *Streptomyces longisporoflavus*. 3 Biotech. 2021 Feb;11(2):51. doi: 10.1007/s13205-020-02547-0, PMID 33489670.
9. Sanam R, Vadivelan S, Tajne S, Narasu L, Rambabu G, Jagarlapudi SA. Discovery of potential ZAP-70 kinase inhibitors: pharmacophore design, database screening and docking studies. Eur J Med Chem. 2009 Dec;44(12):4793-800. doi: 10.1016/j.ejmech.2009.07.018, PMID 19674816.
10. Kandeel M, Kitade Y. Computational analysis of siRNA recognition by the Ago2 PAZ domain and identification of the determinants of RNA-induced gene silencing. PLOS ONE. 2013;8(2):e57140. doi: 10.1371/journal.pone.0057140, PMID 23441235.
11. Duan S, Guan X, Lin R, Liu X, Yan Y, Zhang T, Chen X, Huang J, Sun X, li Q, Fang S, Xu J, Yao Z, Gu H. Silibinin inhibits acetylcholinesterase activity and amyloid β peptide aggregation: a dual-target drug for the treatment of Alzheimer's disease. Neurobiol Aging. 2015 May;36(5):1792-807.
12. Gerometta E, Grondin I, Smadja J, Frederich M, Gauvin Bialecki A. A review of traditional uses, phytochemistry and pharmacology of the genus Indigofera. J Ethnopharmacol. 2020 May 10;253:112608. doi: 10.1016/j.jep.2020.112608, PMID 32004627.
13. Sathish R, Vyawahare B, Natarajan K. Antiulcerogenic activity of lantana camara leaves on gastric and duodenal ulcers in experimental rats. J Ethnopharmacol. 2011 Mar 8;134(1):195-7. doi: 10.1016/j.jep.2010.11.049, PMID 21129476.
14. Abubakar AR, Haque M. Preparation of medicinal plants: basic extraction and fractionation procedures for experimental purposes. J Pharm Bioallied Sci. 2020 Jan-Mar;12(1):1-10. doi: 10.4103/jpbs.JPBS_175_19, PMID 32801594.
15. Hsu KC, Chen YF, lin SR, Yang JM. iGEMDOCK: a graphical environment of enhancing GEMDOCK using pharmacological interactions and post-screening analysis. BMC Bioinformatics. 2011 Feb 15;12 Suppl 1:S33.
16. Duran Iturbide NA, Diaz Eufracio BI, Medina-Franco JL. *In silico* ADME/Tox profiling of natural products: a focus on biofacquim. ACS Omega. 2020 Jun 25;5(26):16076-84. doi: 10.1021/acsomega.0c01581, PMID 32656429.
17. Wallace AC, laskowski RA, Thornton JM. lIGPLOT: a program to generate schematic diagrams of protein-ligand interactions. Protein Eng. 1995 Feb;8(2):127-34. doi: 10.1093/protein/8.2.127, PMID 7630882.
18. Sachdeo R, Khanwelkar C, Shete A. In silico exploration of berberine as a potential wound healing agent via network pharmacology, molecular docking, and molecular dynamics simulation. Int J App Pharm. 2023 Feb;16(2):188-94. doi: 10.22159/ijap.2024v16i2.49922.
19. Gao J, Wang L, Gao C, Arakawa H, Perry G, Wang X. TDP-43 inhibitory peptide alleviates neurodegeneration and memory loss in an APP transgenic mouse model for Alzheimer's disease. Biochim Biophys Acta Mol Basis Dis. 2020 Jan 1;1866(1):165580. doi: 10.1016/j.bbadis.2019.165580, PMID 31678156.
20. Arif R, Ahmad S, Mustafa G, Mahrosh HS, Ali M, Tahir Ul Qamar M. Molecular docking and simulation studies of antidiabetic agents devised from hypoglycemic polypeptide-P of *Momordica charantia*. BioMed Res Int. 2021 Sep 17;2021:5561129. doi:

10.1155/2021/5561129, PMID 34589547.
21. Dominguez Villa FX, Duran Iturbide NA, Avila Zarraga JG. Synthesis, molecular docking, and in silico ADME/Tox profiling studies of new 1-aryl-5-(3-azidopropyl)indol-4-ones: potential inhibitors of SARS CoV-2 main protease. Bioorg Chem. 2021 Jan;106:104497. doi: 10.1016/j.bioorg.2020.104497, PMID 33261847.
22. Nair SS, Varkey J. Isolation of phytoconstituent, *in vitro* anticancer study in hela and MCF-7 CELL lines and molecular docking studies of *Pothos scandens linn*. Int J Curr Pharm Sci. 2021 Sep;13(5):42-51. doi: 10.22159/ijcpr.2021v13i5.1882.
23. Wallace AC, Laskowski RA, Thornton JM. lIGPLOT: a program to generate schematic diagrams of protein-ligand interactions. Protein Eng. 1995 Feb;8(2):127-34. doi: 10.1093/protein/8.2.127, PMID 7630882.
24. Breijyeh Z, Karaman R. Comprehensive review on Alzheimer's disease: causes and treatment. Molecules. 2020 Dec 8;25(24):5789. doi: 10.3390/molecules25245789, PMID 33302541.
25. Chauhan N, Wang KC, Wegiel J, Malik MN. Walnut extract inhibits the fibrillization of amyloid beta-protein and also defibrillizes its preformed fibrils. Curr Alzheimer Res. 2004 Aug;1(3):183-8. doi: 10.2174/1567205043332144, PMID 15975066.
26. Sri Satya MS, Aiswariya BV. Molecular docking and admet studies of ethanone, 1-(2-hydroxy-5-methylphenyl) for antimicrobial properties. Int J Pharm Pharm Sci. 2022 Jun;14(6):24-7.
27. Doody RS, Stevens JC, Beck C, Dubinsky RM, Kaye JA, Gwyther L. Practice parameter: management of dementia (an evidence-based review). Report of the Quality Standards Subcommittee of the American Academy of Neurology. Neurology. 2001 May 8;56(9):1154-66. doi: 10.1212/wnl.56.9.1154, PMID 11342679.
28. Kurian T. Molecular docking study of epigallocatechin gallate on FLT3 in complex with gilteritinib for anticancer activity. Asian J Pharm Clin Res. 2024 Jan;17(1):5-7. doi: 10.22159/ajpcr.2024.v17i1.48733.
29. Grossberg GT. Cholinesterase inhibitors for the treatment of Alzheimer's disease: getting on and staying on. Curr Ther Res Clin Exp. 2003 Apr;64(4):216-35. doi: 10.1016/S0011-393X(03)00059-6, PMID 24944370.
30. Madriwala B, Jays J, Sai GC. Molecular docking and computational pharmacokinetic study of some novel coumarin–benzothiazole schiff's base for antimicrobial activity. Int J Pharm Pharm Sci. 2022 Aug;14(8):16-21. doi: 10.22159/ijpps.2022v14i8.45046.
31. Konappa N, Udayashankar AC, Krishnamurthy S, Pradeep CK, Chowdappa S, Jogaiah S. GC-MS analysis of phytoconstituents from *Amomum nilgiricum* and molecular docking interactions of bioactive serverogenin acetate with target proteins. Sci Rep. 2020 Oct 2;10(1):16438. doi: 10.1038/s41598-020-73442-0, PMID 33009462.